Check for updates
Natural Product Sciences
30(1) : 14-19 (2024)
https://doi.org/10.20307/nps.2024.30.1.14

Ursane-type Triterpene Glycosides from *Rubus cochinchinensis* Exhibited Insulin-Mimetic Activities in Differentiated 3T3-L1 Adipocytes

Jin Pyo An[1,†], Eun Jin Park[1,†], Thi Phuong Doan[1], Byeol Ryu[1], Ha Thanh Tung Pham[2], and Won Keun Oh[1,*]

[1]*Korea Bioactive Natural Material Bank, College of Pharmacy and Research Institute of Pharmaceutical Sciences, Seoul National University, Seoul 08826, Republic of Korea*
[2]*Faculty of Pharmacy, PHENIKAA University, Hanoi 12116, Vietnam*

Abstract – Diabetes mellitus is characterized by hyperglycemic due to impaired insulin secretion or resistance. In our search for anti-diabetic agents, we found that a 70% EtOH extract of *Rubus cochinchinensis* (Tratt) enhances glucose uptake in 3T3-L1 adipocytes. *R. cochinchinensis* is predominantly found in East Asia, particularly in Vietnam, Laos, Cambodia, and southern in China. Despite its widespread distribution, there have been few studies on its bioactivity or chemical constituents. In this study, activity-guided fractionation of 70% EtOH extract from the leaves of *R. cochinchinensis* resulted in the isolation of one new ursane-type glycoside, 3-*O*-*β*-acetyl-28-*O*-*β*-D-glucopyranosyl-rotundioic acid (**1**), along with four known compounds (**2**–**5**). The structures of these compounds were elucidated using 1D and 2D NMR and HRESIMS data. Notably, compound **4** significantly increased the uptake level of 2-deoxy-2-[(7-nitro-2,1,3-benzoxadiazol-4-yl)amino]-D-glucose (2-NBDG) in differentiated 3T3-L1 adipocytes. This study suggests the potential of *R. cochinchinensis* as a promising medicinal plant for treating diabetes via glucose uptake.
Keywords – *Rubus cochinchinensis*, Terpenoids, Ursane-type triterpene glycosides, Anti-diabetes, Glucose uptake

Introduction

Diabetes mellitus is a widespread metabolic disorder characterized by chronic hyperglycemia and is divided into type 1 and type 2 diabetes mellitus.[1] Insulin-dependent type 1 diabetes mellitus (T1DM) is primarily associated with the damage of pancreatic *β*-cells, leading to the absence of insulin production. Type 2 diabetes mellitus (T2DM), which is insulin-independent, arises mainly from insulin resistance. This disease has become a major global health concern, threatening the health of numerous individuals.[2] The number of T2DM patients has tripled from 1980 to 2017, increasing to 425 million. It is expected to reach 629 million by 2045, accounting for 90% of all diabetes cases worldwide.[3] In 2015, the expenditure for diabetes-related amounted to 1,300 billion dollars, which represented 1.8% of the global GDP.[4] If this trend continues, T2DM will pose a significant public health threat accompanied by an increasing social-economic burden. Therefore, developing effective, affordable anti-diabetic agents and reducing the incidence of T2DM has become a crucial task in modern healthcare.

Impaired glucose metabolism is a major pathological characteristic of T2DM and obesity. Maintaining a balance between glucose uptake in peripheral tissues and glucose production in the liver is pivotal for glucose homeostasis.[5] The glucose transporter 4 (GLUT4) protein plays a vital role in mediating glucose uptake and regulating systemic glucose homeostasis in response to insulin. It is mainly expressed in adipose tissue and skeletal muscle.[6] In these tissues, reduced GLUT4 protein expression or impaired translocation of the protein leads to diminished glucose uptake.[7,8] These results in elevated blood glucose levels, ultimately contributing to the development of T2DM. Therefore, enhancing glucose uptake in peripheral tissues is an effective therapeutic strategy to reduce blood glucose levels and manage T2DM.[9]

Natural products serve as important sources of therapeutic agents for enhancing glucose uptake, and many studies have identified triterpenoids as potential candidates. For instance, corosolic acid, found in *Lagerstroemia specios* L., has been shown to improve hyperglycemia following oral sucrose administration and significantly

*Author for correspondence
Won Keun Oh, Korea Bioactive Natural Material Bank, College of Pharmacy and Research Institute of Pharmaceutical Sciences, Seoul National University, Seoul 08826, Republic of Korea
Tel: +82-2-880-7872; E-mail: wkoh1@snu.ac.kr

†These authors contributed equally to this work.

reduce sucrose hydrolysis in the small intestine of mice.[10] Ursolic acid, isolated from cornelian cherries, increased insulin levels in glucose intolerance-induced mice on a high-fat diet.[11] Tormentic acid, a natural compound from *Peterium ancistroides*, not only lowered fasting plasma glucose levels but also increased circulating insulin levels, thereby improving glucose tolerance by enhancing the insulin secretory response to glucose.[12] Recently, triterpenoid saponins isolated from *Pericampylus glaucs* have been found to stimulate glucose uptake in differentiated 3T3-L1 adipocyte.[13]

In this study, plant extracts from the Korea Bioactive Natural Material Bank (KBNMB) were screened for their anti-diabetic activities, focusing on 2-NBDG uptake in differentiated 3T3-L1 adipocytes. The 70% EtOH extract of *R. cochinchinensis*, a member of the Rosaceae family, exhibited significant enhancing activity on glucose uptake. *R. cochinchinensis* is a climbing shrub that produces numerous stems from a ligneous rootstock and is widely distributed in Vietnam, southern China, Laos, and Cambodia. Its fruit is edible and locally consumed in Vietnam. Despite this usage, there has been limited research on its chemical properties, with only one study reported and no published reports on its bioactivity.[14] Therefore, our study focused on identifying the chemical constituents and bioactivity of this plant. Through successive chromatographic procedures with silica gel, RP-C18, and HPLC, one new ursane-type triterpenoid (**1**) and four known compounds (**2**–**5**) were isolated from a 70% EtOH extract of the *R. cochinchinensis* (Fig. 1). All isolated compounds (**1**–**5**) were then evaluated for their glucose uptake levels in differentiated 3T3-L1 adipocytes using 2-deoxy-2-[(7-nitro-2,1,3-benzoxadiazol-4-yl)amino]-D-glucose (2-NBDG).

Experimental

General experimental procedures – Optical rotations were measured using a JASCO P-2000 polarimeter (JASCO International Co. Ltd., Tokyo, Japan). Infrared (IR) spectroscopic data were acquired with a Nicolet 6700 FT-IR spectrometer (Thermo Fisher Scientific, Waltham, MA, USA). High-resolution electrospray ionization mass spectrometry (HRESIMS) data were collected using an Agilent 6530 Q-TOF mass spectrometer, coupled with an Agilent 1260 Infinity HPLC (Agilent Technologies, Santa Clara, CA, USA). Nuclear magnetic resonance (NMR) spectra were recorded on a Bruker Avance-800 spectrometer (Billerica, MA, USA). Column chromatography was performed using silica gel (63–200 μm, Merck, Darmstadt, Germany), reverse-phase C18 (RP-C18, 40–63 μm, Merck), and Sephadex LH-20 (Sigma-Aldrich, St. Louis, MO, USA). High performance liquid chromatography (HPLC) analyses were conducted on a Gilson HPLC system equipped with an Optima Pak C18 column (10 mm × 250 mm, 10 μm; RS Tech, Seoul, Korea). Analytical-grade solvents were used for isolation and analysis, while industrial-grade solvents were employed for extraction processes (Daejung Chemicals & Metals Co. Siheung, Korea).

Plant material – *Rubus cochinchinensis* (Rosaceae) was collected in Hanoi city, Vietnam, in November 2017. The plant sample was authenticated by Dr. H. T. T. Pham at PHENIKAA University in Vietnam. A voucher specimen (SNU2017-0058) has been deposited at the Medicinal Herbarium of the College of Pharmacy, Seoul National University, Seoul, Korea.

Extraction and isolation – Dried leaves of *R. cochinchinensis* (800 g) were extracted three times over 6 h with 70% EtOH, using sonication at room temperature. The extract was then concentrated under reduced pressure to obtain a dried sample (80 g). This concentrated extract was suspended in H_2O and successively partitioned with *n*-hexane, EtOAc, and *n*-BuOH. The EtOAc fraction (21 g) was subjected to Sephadex LH-20 column chromatography with a MeOH/H_2O system (7:3), yielding three subfractions (Frs. 2.1–2.3). Fr. 2.2 (5 g) was further chromatographed on a RP-18 column (4.5 × 40 cm; 150 μm particle size) using a MeOH/H_2O system (7:13 to 20:0), resulting in 11 sub-fractions (Frs. 2.2.1–2.2.11). Fr. 2.2.8 (150 mg) was purified by HPLC [(Gilson system, Optima Pak C18 column (10 × 250 mm, 10 μm particle size), mobile phase MeCN/H_2O (29:71, v/v), flow rate 3 mL/min; UV detector wavelengths at 201 and 254 nm)] to obtain compounds **1** (3.5 mg; t_R = 34.2 min), **3** (6.0 mg; t_R = 37.0 min), and **4** (4.5 mg; t_R = 19.4 min). Fr. 2.8 (120 mg) was separated using HPLC [(Gilson system, Optima Pak C18 column (10 × 250 mm, 10 μm particle size, mobile phase MeCN/H_2O (21:79, v/v), flow rate 3 mL/min; UV detector wavelengths at 201 and 254 nm) to yield compound **2** (6.5 mg; t_R = 43.0 min). Fr. 2.2.6 (100 mg) was further purified by HPLC using a Gilson system equipped with an Optima Pak C18 column (10 × 250 mm, 10 μm particle size). The mobile phase consisted of MeCN/H_2O (29:71, v/v), with a flow rate of 3 mL/min. The UV detector was set at wavelengths at 201 and 254 nm) to yield compound **5** (4.5 mg; t_R = 43.0 min).

3-*O*-*β*-acetyl-28-*O*-*β*-D-glucopyranosyl-rotundioic acid (1) – White amorphous powder; $[\alpha]_D^{25}$ + 20 (*c* 0.2, MeOH); IR (KBr) ν_{max}; 3394, 2930, 1733, 1569, 1050 cm^{-1}; UV (MeOH) λ_{max} (log ε) 200 (4.23) nm; ^1H and ^{13}C NMR spectral data, see Table 1; HRESIMS *m/z* 745.3803 [M+

Na]$^+$ (calcd for $C_{38}H_{58}O_{13}Na$, 745.3775, mass error 3.75 ppm).

Acid hydrolysis for sugar determination – Compound **1** (2.0 mg) underwent hydrolysis using 2 mL of 2N HCl (H_2O/ethylene oxide, 1:1) at 100 ºC for 3 h. The resulting solution was then dried, re-suspended in H_2O, and partitioned with EtOAc. The H_2O layer was subsequently dried and dissolved in 1.0 mL of pyridine, to which 1.5 mg of L-cysteine methyl ester hydrochloride was added. This mixture was incubated for 2 h at 60 ºC, followed by the addition of 0.2 mL of trimethylsilylimidazole and further incubated for another 2 h at 60 ºC. After drying, the mixture was partitioned between H_2O (2.0 mL) and *n*-hexane (2.0 mL). The sugar unit in compound **1** exhibited a retention time of 12.18 min, closely matching the retention time of 12.20 min for the trimethylsilyl-L-cysteine derivatives derived from authentic D-glucose. This correlation was observed under identical UHPLC conditions using a YMC RP C18 column (250 × 4.6 i.d., 5 μM, YMC Co., Ltd., Japan), UV detection at 250 nm, a flow rate of 1.0 mL/min, and a gradient system of 10–90% MeCN/H_2O (0.1% formic acid) over 20 min. This was followed by a 4 min washing step at 100% MeCN and a subsequent 4 min re-stabilization period at 10% MeCN/H_2O.

Differentiation of 3T3-L1 preadipocytes – 3T3-L1 preadipocyte cells were cultured in Dulbeco's Modified Eagle's Medium (DMEM, Hyclone, UT, USA) supplemented with 10% calf serum, 100 U/mL penicillin, and 100 mg/mL streptomycin (Hyclone). The cells were incubated in an environment of 5% CO_2 at 37 ºC. Two days post-incubation, the growth medium was replaced with DMEM containing 10% fetal bovine serum (FBS) (Hyclone), 1 μM dexamethasone (Sigma, MO, USA), 0.52 mM 3-isobutyl-1-methylxanthine (Sigma), and 1 μg/ mL insulin (Roche, Germany). After 48 h, the cells were maintained in DMEM with 10% FBS, 1 μg/ mL insulin, 100 U/mL penicillin, and 100 mg/mL streptomycin for an additional 2 days. The medium was subsequently replaced with DMEM supplemented with 10% FBS every two days until complete adipogenesis was induced.

Glucose uptake assay – To measure glucose uptake, the fluorescent glucose derivative, 2-deoxy-2-[(7-nitro-2,1,3-benzoxadiazol-4-yl)amino]-D-glucose (2-NBDG, Invitrogen, Eugene, OR, USA), was utilized in vitro. Briefly, 3T3-L1 adipocytes were cultured on 96-well plates in a glucose-free medium containing 10% FBS, as previously described.[13] After a 24 h incubation, the cells were treated with insulin (as a positive control) and test compounds in the presence or absence of 2-NBDG. The cultures were then incubated for an additional 1 h, and the cells were then washed with cold phosphate-buffered saline (PBS). To quantify the fluorescence of 2-NBDG, the signal intensity was measured at excitation/emission wavelengths of 450/535 nm using a fluorescence microplate reader (Spectra Max Gemini XPS, Molecular Devices, San Jose, CA, USA). For visual analysis of 2-NBDG transport into the cells, 3T3-L1 adipocytes were seeded on sterilized glass coverslips in glucose-free medium containing 10% FBS for 24 h. After the treatments and incubation, the cells were washed with cold PBS and fluorescent images were captured using a fluorescence microscope (Olympus ix70, Olympus Corporation, Tokyo, Japan).

Results and Discussion

The physical and spectral properties of the known compounds (**2**–**5**) were compared with those reported in previous literature. Based on this comparison, they were identified as suavissimoside F1 (**2**)[15], 2-*O*-acetyl suavissimoside F1 (**3**)[14], ilexoside XXVII (**4**)[16], and ilexoside XXX (**5**)[17] (Fig. 1).

Compound **1** was obtained as a white amorphous powder, exhibiting a specific rotation of $[\alpha]_D^{25}$ + 20 (*c* 0.2, MeOH). Its molecular formula was deduced as $C_{38}H_{58}O_{13}$ based on the protonated high-resolution electrospray ionization mass spectrometry (HRESIMS) ion peak at *m/z* 745.3803 (calcd for $C_{38}H_{58}O_{13}Na$, 745.3775), indicating ten degrees of unsaturation. The infrared (IR) spectrum displayed absorptions characteristic of hydroxy (3394 cm^{-1}), carboxyl (1733 cm^{-1}), and olefinic (1569 cm^{-1}) functional groups. The ^{1}H NMR spectrum of compound **1** showed typical signals of an ursane-type skeleton. These included one olefinic (δ_H 5.54, 1H, t, J = 3.4 Hz), two oxymethines

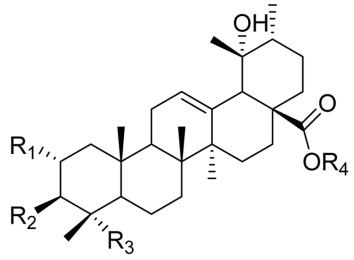

	R_1	R_2	R_3	R_4
1	OH	OAc	COOH	*O*-*β*-D-glc
2	OH	OH	COOH	*O*-*β*-D-glc
3	OAc	OH	COOH	*O*-*β*-D-glc
4	H	*O*-*α*-L-ara	CH_2OH	*O*-*β*-D-glc
5	H	OH	COOH	*O*-*β*-D-glc

Fig. 1. Chemical structures of compounds **1**–**5** isolated from *R. cochinchinensis*.

Table 1. ^{1}H and ^{13}C NMR spectroscopic data for new compound **1**

Position	**1**		
	δ_C, type		δ_H (J in Hz)
1	49.1,	CH_2	2.36 (dd, 12.6, 4.3), 1.54 (m)
2	66.9,	CH	4.36 (td, 10.6, 4.1)
3	82.7,	CH	6.05 (d, 9.8)
4	53.7,	C	-
5	52.0,	CH	2.37 (m)
6	21.9,	CH_2	1.71 (m), 1.57 (m)
7	33.5,	CH_2	1.83 (m), 1.45 (br d, 12.3)
8	41.0,	C	-
9	48.4,	CH	2.09 (m)
10	38.5,	C	-
11	24.4,	CH_2	2.13 (m), 2.12 (m)
12	128.4,	CH	5.54 (t, 3.4)
13	139.7,	C	-
14	42.5,	C	-
15	29.5,	CH_2	2.46 (m), 1.18 (m)
16	26.4,	CH_2	3.08 (td, 13.1, 4.4), 1.99 (m)
17	48.9,	C	-
18	54.8,	CH	2.93 (s)
19	73.0,	C	-
20	42.5,	CH	1.33 (m)
21	27.1,	CH_2	2.00 (m), 1.23 (m)
22	38.1,	CH_2	2.05 (dt, 13.0, 3.3), 1.85 (td, 13.2, 4.2)
23	179.1,	CH_2	-
24	14.2,	CH_3	1.64 (3H, s)
25	17.6,	CH_3	1.15 (3H, s)
26	17.7,	CH_3	1.22 (3H, s)
27	24.9,	CH_3	1.65 (3H, s)
28	177.3,	C	-
29	27.3,	CH_3	1.39 (3H, s)
30	17.1,	CH_3	1.08 (3H, d, 6.0)
1′	96.2,	CH	6.32 (d, 7.9)
2′	74.4,	CH	4.25 (t, 8.6)
3′	79.4,	CH	4.33 (t, 8.9)
4′	71.6,	CH	4.40 (t, 9.2)
5′	79.7,	CH	4.08 (ddd, 9.6, 4.4, 2.6)
6′	62.7,	CH_2	4.51 (dd, 11.9, 2.4), 4.44 (dd, 11.9, 4.5)
AcO	170.7,	C	
	21.5,	CH_3	1.99 (3H, s)

(δ_H 4.36, 1H, td, J = 10.6, 4.1 Hz and δ_H 6.05, 1H, d, J = 9.8 Hz), one doublet methyl (δ_H 1.08, 3H, d, J = 6.0 Hz), five singlet methyls (δ_H 1.65, 1.64, 1.39, 1.22, 1.15, all s, each 3H), and one anomeric proton (δ_H 6.32, 1H, d, J = 7.9 Hz) (Table 1). The ^{13}C NMR spectrum revealed signals for 38 carbons, including an olefinic group (δ_C 139.7 and 128.4), two carbonyl groups (δ_C 179.1 and 177.3), one acetyl group (δ_C 170.7 and 21.5), and one oxygenated quaternary carbon (δ_C 73.0) (Table 1). Analysis of the HMBC data for compound **1** indicated the presence of glucopyranosyl moiety at C-28, as evidenced by the key correlation from H-1' (δ_H 6.32) to C-28 (δ_C 177.3) (Fig. 2A). An acetyl group attachment at C-3 in compound **1** was confirmed based on the HMBC correlation from H-3 (δ_H 6.05) of the aglycone to the carbonyl carbon (δ_C 170.7) (Fig. 2A). The NMR data for compound **1** closely resembled those of suavissimoside F1, previously isolated from *R. cochinchinensis*.[15] The major difference in compound **1** was the acetylation at C-3, where the chemical shift of C-3 (δ_C 82.7) was observed at a lower field compared to that of suavissimoside F1 (δ_C 80.9). Additionally, the large coupling constant (J = 7.9 Hz) associated with the anomeric proton signal, coupled with the carbon data at δ_C 96.2, provided evidence supporting the presence of a β-linked glucose moiety at C-28.[18,19] The absolute configuration of the 28-glucopyranosyl moiety in **1** was subsequently validated as D-glucose through an acid hydrolysis, followed by derivatization with L-cysteine methyl ester and *O*-tolyl isothiocyanate. The confirmation was further substantiated by comparing the retention time (RT) of the sugar derivative with that of an authentic D-glucose standard.[20] As a result, the RT values for the sugar derivatives were recorded as 12.18 for compound **1** and 12.20 min for the authentic sugar, respectively. The *trans* orientation of H-2 and H-3 in compound **1** were determined by analyzing the coupling constants of H-2 (δ_H 4.36, td, J = 10.6, 4.1 Hz) and H-3 (δ_H 6.05, d, J = 9.8 Hz). As shown in Fig. 2B, the ROESY correlations between H-2/Me-25, and H-2/Me-23 indicated a 2α, 19α-dihydroxy configuration. Additionally, correlations involving H-18/Me-29 and H-20/Me-29 suggested the presence of 19α-hydroxyl and 30α-methyl groups, respectively, on the ursane-type skeleton. The identification of 3β-acetyl and 28β-glucopyranosyl moieties was further inferred from the cross-peak observed between Me-26 and H-1', as illustrated in Fig. 2B. Therefore, compound **1** was characterized as 3-*O*-β-acetyl-28-*O*-β-D-glucopyranosyl-rotundioic acid.

Insulin mimetics derived from natural products have been considered as potential therapeutic agents due to their ability to penetrate the blood-brain barrier and their generally fewer side effects compared to synthesized reagents.[21] 2-NBDG, a fluorescent-tagged glucose probe, is used to monitor glucose uptake. To assess the insulin mimetic activities of all isolates (**1**–**5**) from *R. cochinchinensis*, intracellular glucose levels were measured by

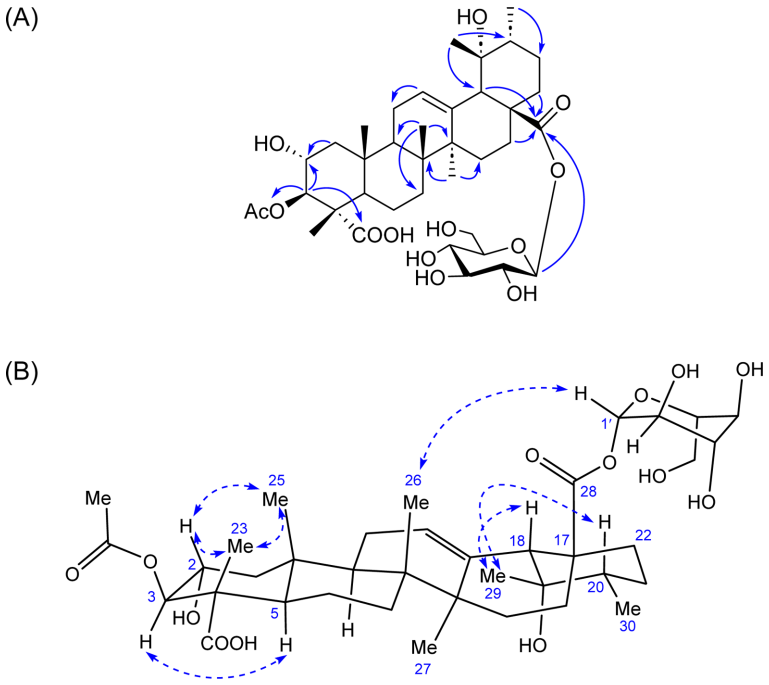

Fig. 2. (A) Selected HMBC correlations (blue arrows) and (B) selected ROESY correlations (dashed blue arrows) for compound **1**.

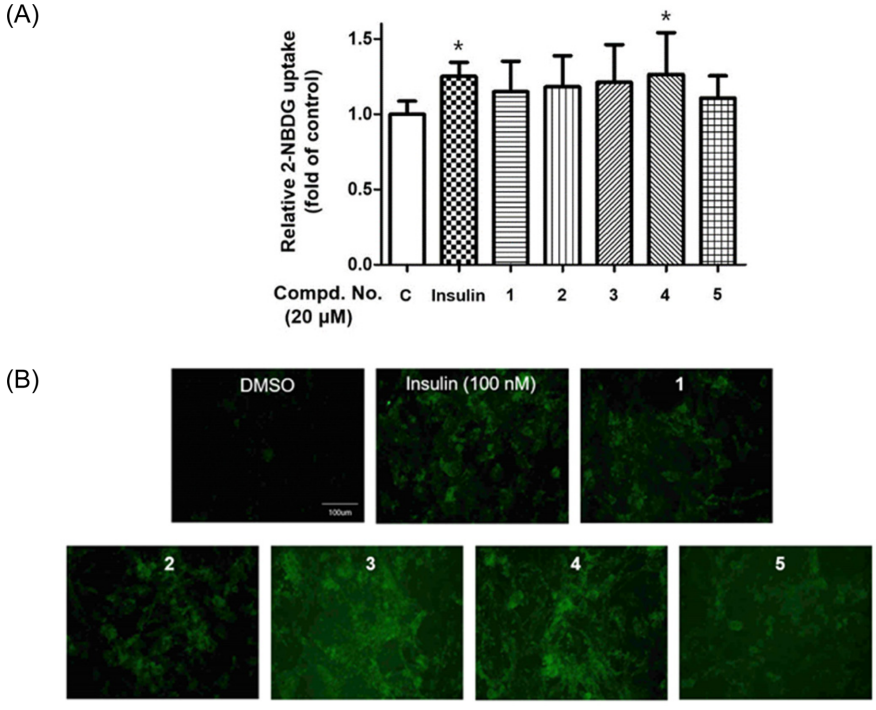

Fig. 3. Stimulation effects of compounds **1**–**5** on glucose uptake in 3T3-L1 adipocytes using a fluorescent analog of glucose (2-NBDG). (A) 3T3-L1 adipocytes were treated with 100 nM insulin and test compounds for 1 h in the presence of 2-NBDG. The glucose uptake was measured at excitation/emission (ex/em) wavelengths of 450/535 nm using a fluorescence microplate reader. The results were expressed as means ± SD ($n = 3$), with each experiment conducted in triplicate. Significant differences between groups were determined using the one-way analysis of variance (ANOVA) with the GraphPad Prism system. The asterisk (*) indicates that the p-value of each group compared to the control group is significant. Significance was recognized at $^{*}p < 0.05$, compared to the control group (without treatment). (B) 3T3-L1 adipocytes were incubated with insulin (100 nM) and compounds **1**–**5** (20 μM each) for 1 h. Subsequently, the cells were observed using a fluorescence microscope. The green fluorescent signals, indicating successful transport of 2-NBDG into the cells, were significantly increased.

2-NBDG uptake in differentiated 3T3-L1 adipocytes at a concentration of 20 μM. Among these compounds, compound **4** exhibited a significant glucose uptake effect (Fig. 3A). Fluorescent intensities, indicating increased 2-NBDG uptake in 3T3-L1 adipocytes treated with compound **3** was higher than those in the untreated negative group (Fig. 3B).

While searching for anti-diabetic agents from natural products, we found that a 70% EtOH extract of *R. cochinchinensis* enhances glucose uptake in differentiated 3T3-L1 adipocyte cells. This led us to investigate the chemical profiles of *R. cochinchinensis* by bioactivity-guided isolation. As a result, we isolated five triterpenoid saponins, including one new ursane-type glycoside, 3-*O*-*β*-acetyl-28-*O*-*β*-D-glucopyranosyl-rotundioic acid (**1**), along with four known compounds (**2**–**5**) from a 70% EtOH extract of the leaves of *R. cochinchinensis*. Furthermore, all isolates (**1**–**5**) from *R. cochinchinensis*, were evaluated for their insulin mimetic activities by measuring intracellular glucose levels using 2-NBDG uptake in differentiated 3T3-L1 adipocytes at a concentration of 20 μM. Among these, compounds **3** and **4** demonstrated significant glucose uptake effects.

In this study, we isolated ursane-type triterpenoid saponins from the leaves of *R. cochinchinensis* were isolated and evaluated for their glucose uptake stimulatory effects for the first time. To date, only a few studies have demonstrated that triterpenoids or triterpenoid saponins from natural products have anti-diabetic effects.[10–13] Our findings from this study also consolidated that triterpenoid saponins derived from natural products are potential sources of antidiabetic agents, as in previous studies.

Acknowledgments

This research was supported by grants from the Basic Science Research Program (NRF-2022R1A2C2005061) and (2022M3H9A1082984) through the National Research Foundation of Korea (NRF) funded by the Ministry of Science and ICT in Korea.

Conflicts of interest

The authors declare no potential conflicts of interest with respect to the research, authorship, and/or publication of this article.

References

(1) Zhang, Y.; Zhou, G.; Peng, Y.; Wang, M.; Li, X. *J. Ethnopharmacol*. **2020**, *247*, 112273.
(2) Inzucchi, S. E.; Bergenstal, R. M.; Buse, J. B.; Diamant, M.; Ferrannini, E.; Nauck, M.; Peters, A. L.; Tsapas, A.; Wender, R.; Matthews, D. R. *Diabetes Care* **2015**, *38*, 140–149.
(3) Gomes, M. B.; Rathmann, W.; Charbonnel, B.; Khunti, K.; Kosiborod, M.; Nicolucci, A.; Pocock, S. J.; Shestakova, M. V.; Shimomura, I.; Tang, F.; Watada, H.; Chen, H.; Cid-Ruzafa, J.; Fenici, P.; Hammar, N.; Surmont, F.; Ji, L. *Diabetes Res. Clin. Pract*. **2019**, *151*, 20–32.
(4) Bommer, C.; Sagalova, V.; Heesemann, E.; Manne-Goehler, J.; Atun, R.; Bärnighausen, T.; Davies, J.; Vollmer, S. *Diabetes Care* **2018**, *41*, 963–970.
(5) Seo, H. R.; Lee, A. Y.; Cho, K. M.; Cho, E. J.; Kim, H. Y. *Nat. Prod. Sci.* **2017**, *23*, 61.
(6) Huang, S.; Czech, M. P. *Cell Metab*. **2007**, *5*, 237–252.
(7) Leto, D.; Saltiel, A. R. *Nat. Rev. Mol.Cell Biol*. **2012**, *13*, 383–396.
(8) Krook, A.; Wallberg-Henriksson, H.; Zierath, J. R. *Med. Sci. Sports Exerc*. **2004**, *36*, 1212–1217.
(9) Coughlan, K. A; Valentine, R. J.; Ruderman, N. B.; Saha, A. K. *Diabetes Metab. Syndr. Obes*. **2014**, 241–253.
(10) Takagi, S.; Miura, T.; Ishibashi, C.; Kawata, T.; Ishihara, E.; Gu, Y.; Ishida, T. *J. Nutr. Sci. Vitaminol.* **2008**, *54*, 266–268.
(11) Jayaprakasam, B.; Olson, L. K.; Schutzki, R. E.; Tai, M.-H.; Nair, M. G. *J. Agric. Food Chem*. **2006**, *54*, 243–248.
(12) Ivorra, M. D.; Paya, M.; Villar, A. *Planta Med*. **1988**, *54*, 282–286.
(13) Lee, H.-J.; Cho, H.-M.; Park, E.-J.; Lee, B.-W.; Nghiem, D.-T.; Pham, H.-T.-T.; Pan, C.-H.; Oh, W.-K. *Bioorg. Chem*. **2021**, *117*, 105445.
(14) Lien, T. P.; Kamperdick, C.; Van Sung, T.; Adam, G. *Phytochemistry* **1999**, *50*, 463–465.
(15) Gao, F.; Chen, F.; Tanaka, T.; Kasai, R.; Seto, T.; Tanaka, O. *Chem. Pharm. Bull.* **1985**, *33*, 37–40.
(16) Yano, I.; Nishiizumi, C.; Yoshikawa, K.; Arihara, S. *Phytochemistry* **1993**, *32*, 417–420.
(17) Miyase, S.; Yoshikawa, K.; Arihara, S. *Chem. Pharm. Bull.* **1992**, *40*, 2304–2307.
(18) Tanaka, T.; Nakashima, T.; Ueda, T.; Tomii, K.; Kouno, I. *Chem. Pharm. Bull*. **2007**, *55*, 899–901.
(19) Roslund, M. U.; Tähtinen, P.; Niemitz, M.; Sjöholm, R. *Carbohydr. Res*. **2008**, *343*, 101–112.
(20) Tanaka, T.; Nakashima, T.; Ueda, T.; Tomii, K.; Kouno, I. *Chem. Pharm. Bull.* **2007**, *55*, 899–901.
(21) Qin, Z.; Pandey, N. R.; Zhou, X.; Stewart, C. A.; Hari, A.; Huang, H.; Stewart, A. F. R.; Brunel, J. M.; Chen, H.-H. *Biochem. Biophys. Res. Commun*. **2015**, *458*, 21–27.

Received December 5, 2023
Revised February 29, 2024
Accepted February 29, 2024

SUPPLEMENTARY MATERIAL

Ursane-type Triterpene Glycosides from *Rubus cochinchinensis* Exhibited Insulin-Mimetic Activities in Differentiated 3T3-L1 Adipocytes

Jin Pyo An[1,†], Eun Jin Park[1,†], Thi Phuong Doan[1], Byeol Ryu[1], Ha Thanh Tung Pham[2], and Won Keun Oh[1,*]

[1]Korea Bioactive Natural Material Bank, College of Pharmacy and Research Institute of Pharmaceutical Sciences, Seoul National University, Seoul 08826, Republic of Korea

[2]Faculty of Pharmacy, PHENIKAA University, Hanoi 12116, Vietnam

*Author for correspondence

Tel: +82-02-880-7872; E-mail: wkoh1@snu.ac.kr

†These authors contributed equally to this work.

CONTENTS

Figure S1. ^{1}H NMR spectrum (pyridine-d_5, 800 MHz) of compound **1**

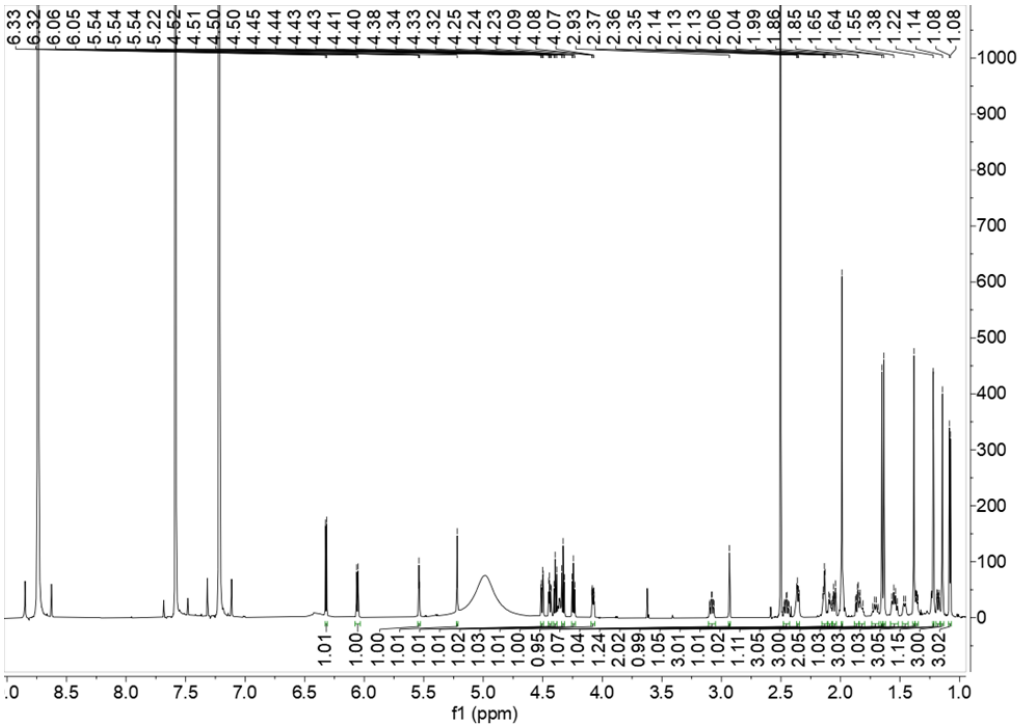

Figure S2. Expand ^{1}H NMR spectrum (pyridine-d_5, 800 MHz) of compound **1**

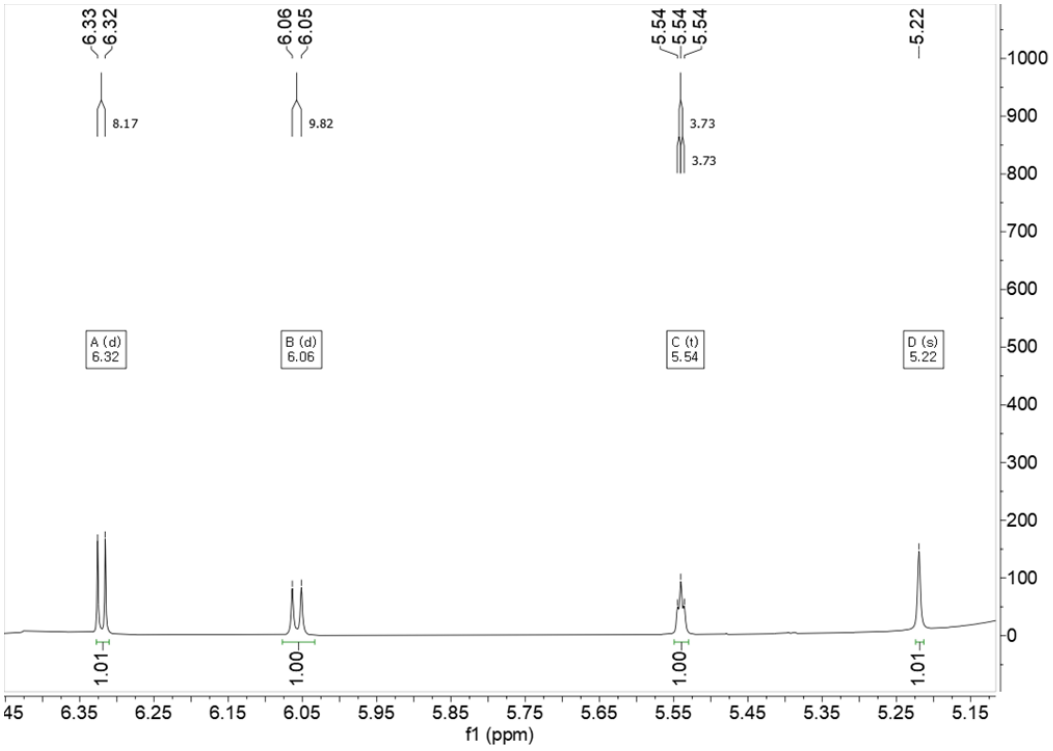

Figure S3. ^{13}C NMR spectrum (pyridine-d_5, 200 MHz) of compound **1**

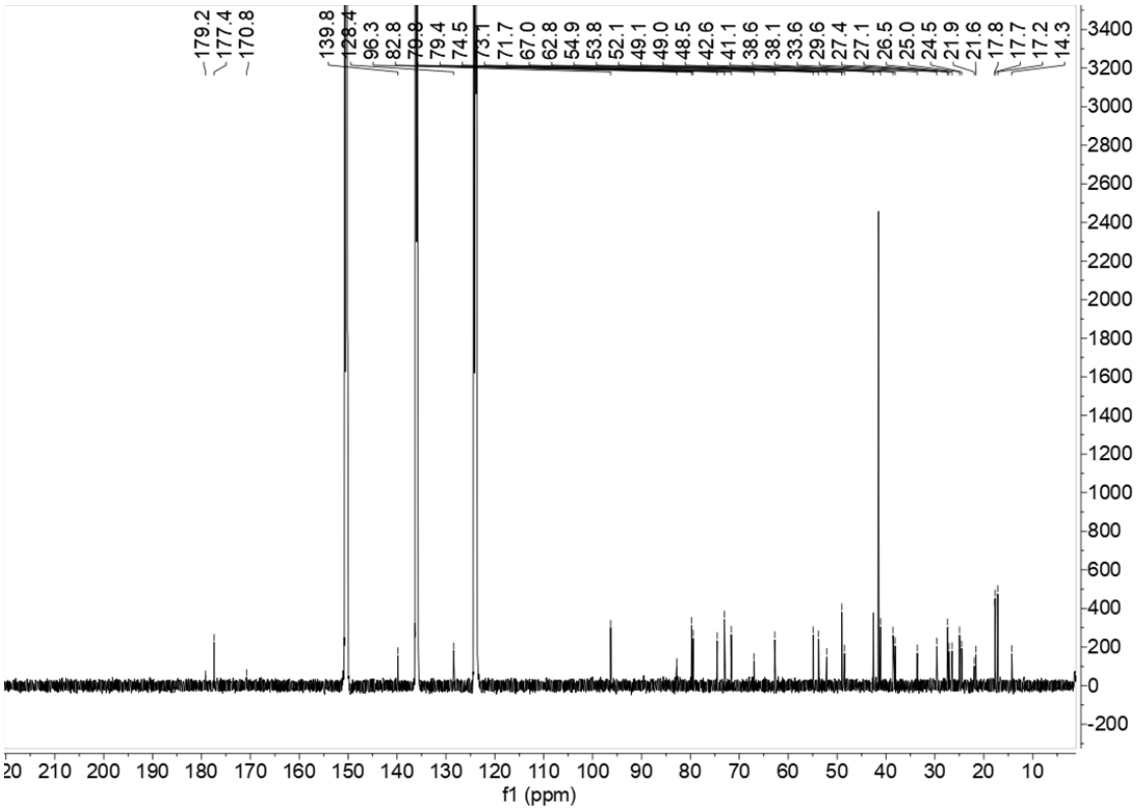

Figure S4. HSQC spectrum (pyridine-d_5, 800 MHz) of compound **1**

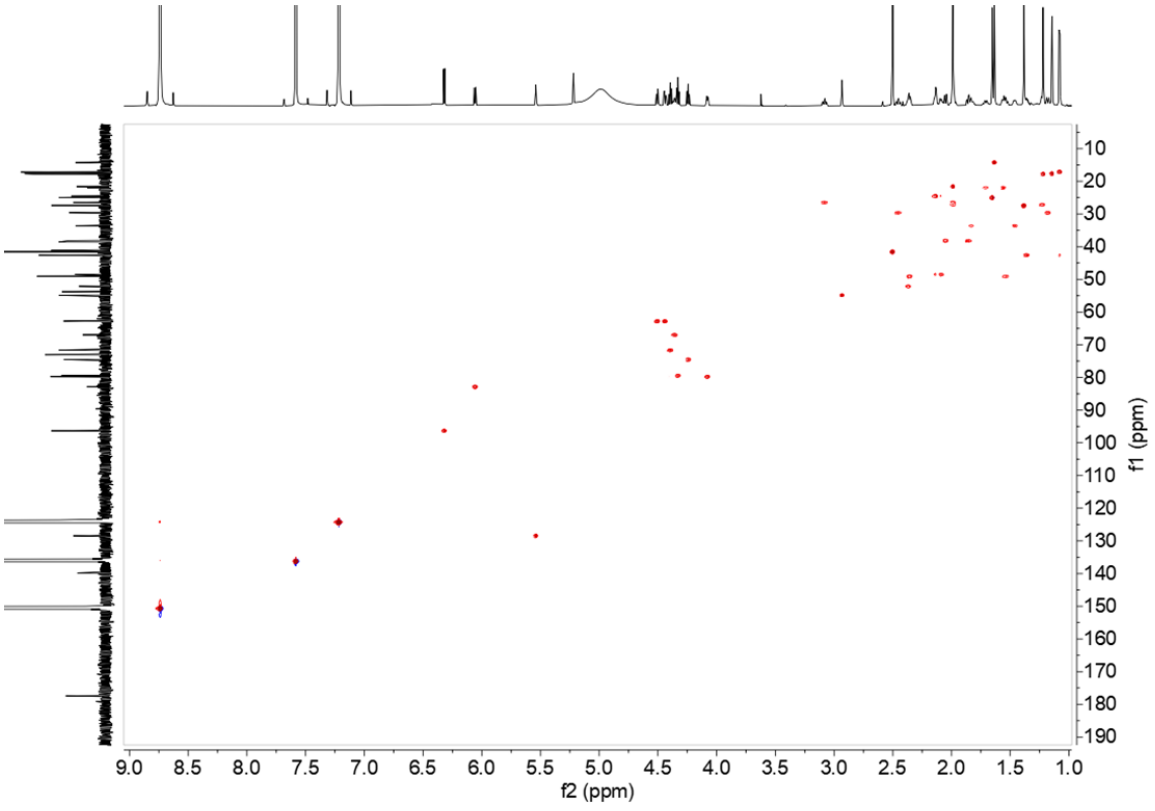

Figure S5. HMBC spectrum (pyridine-d_5, 800 MHz) of compound **1**

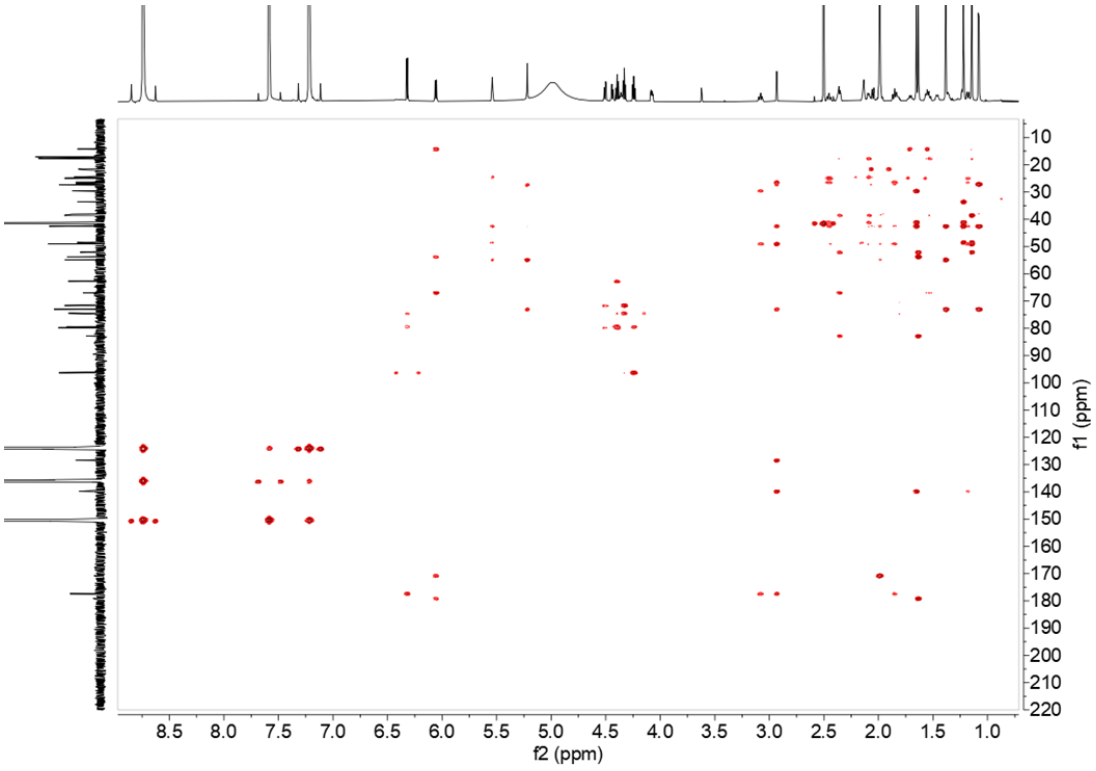

Figure S6. COSY spectrum (pyridine-d_5, 800 MHz) of compound **1**

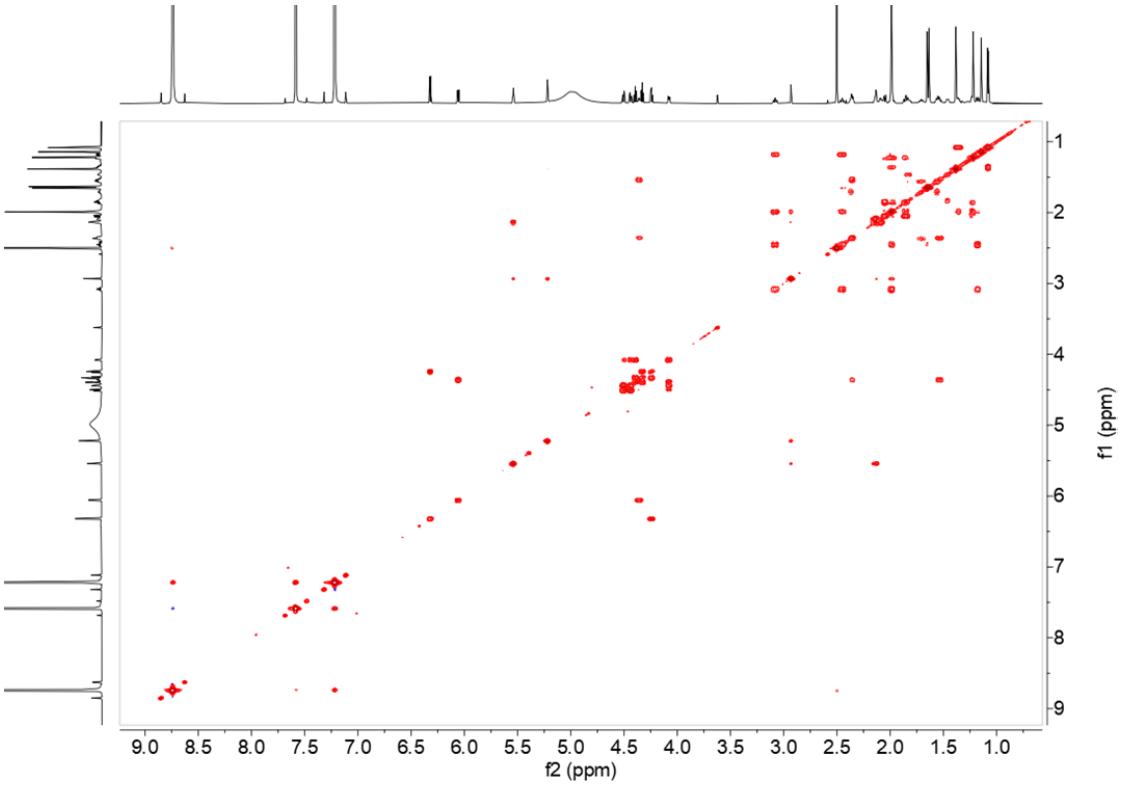

Figure S7. NOESY spectrum (pyridine-d_5, 800 MHz) of compound **1**

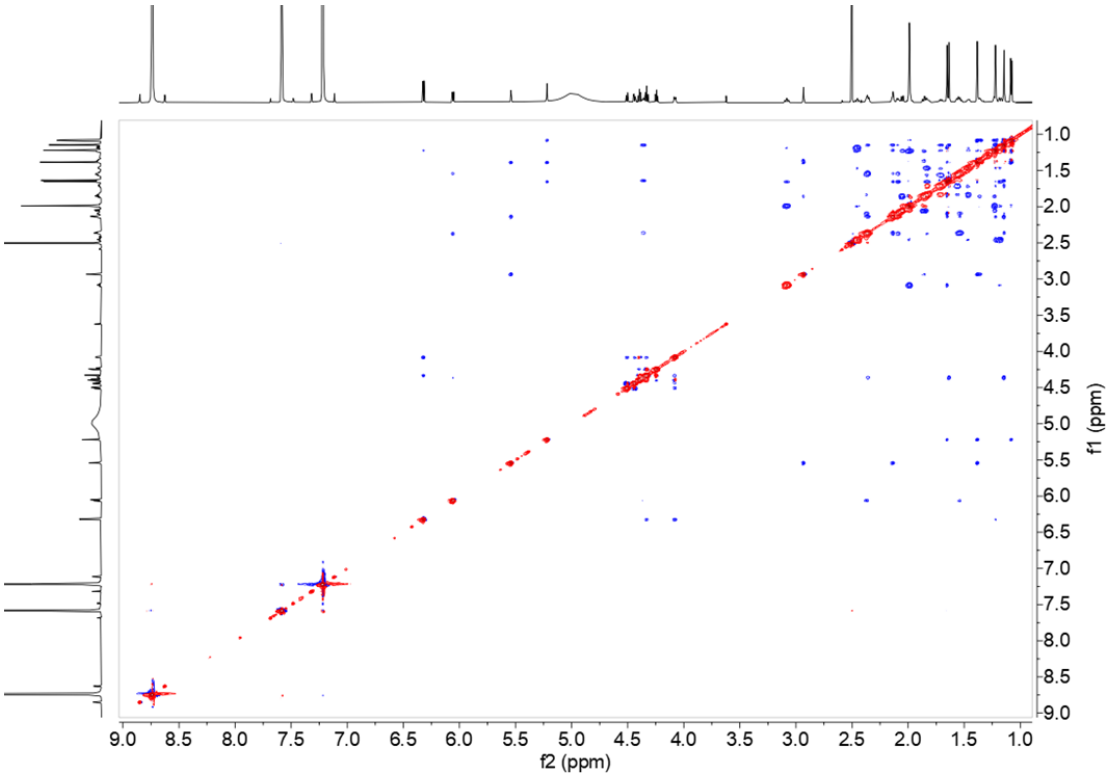

Figure S8. HRESIMS of compound **1**

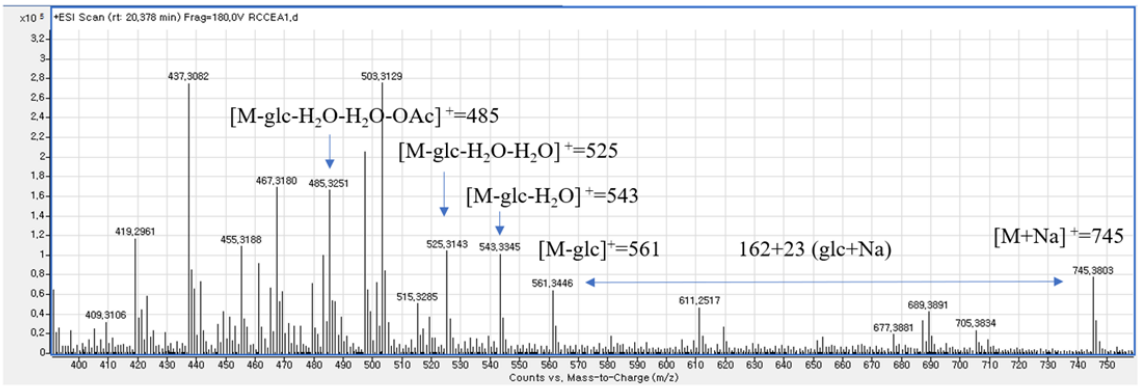

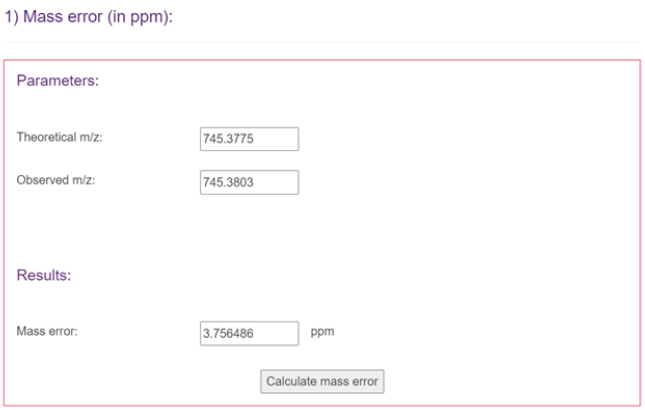

Figure S9. IR spectrum of compound **1**

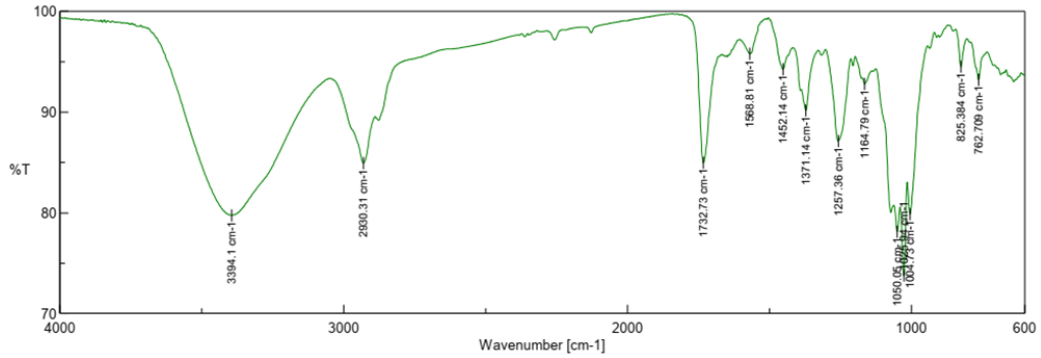

[Comment]
Sample Name rcc1
Comment
User
Division
Company 공동기기실

[Data Information]
Creation Date 2020-08-10 오후 3:14
Data array type Linear data array
Horizontal Wavenumber [cm-1]
Vertical %T
Start 599.753 cm-1
End 4000.6 cm-1
Data pitch 0.964233 cm-1
Data points 3528

[Measurement Information]
Model Name FT/IR-4200typeA
Serial Number B038361018

Light Source Standard
Detector TGS
Accumulation 16
Resolution 4 cm-1
Zero Filling On
Apodization Cosine
Gain Auto (1)
Aperture Auto (7.1 mm)
Scanning Speed Auto (2 mm/sec)
Filter Auto (30000 Hz)

Figure S10. UV spectrum of compound **1**

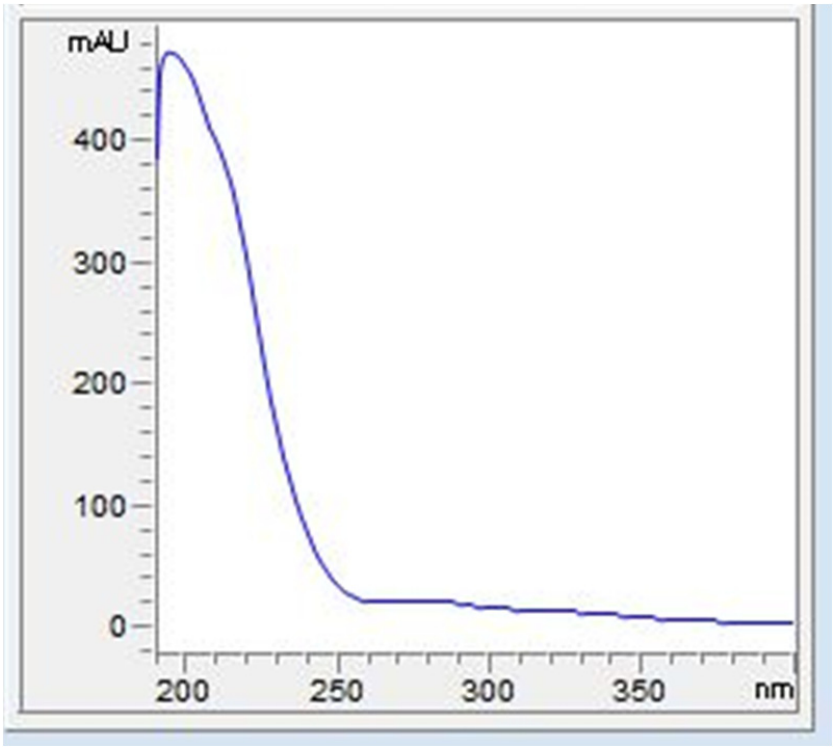

Figure S11. ^{1}H NMR spectrum (pyridine-d_5, 600 MHz) of compound **2**

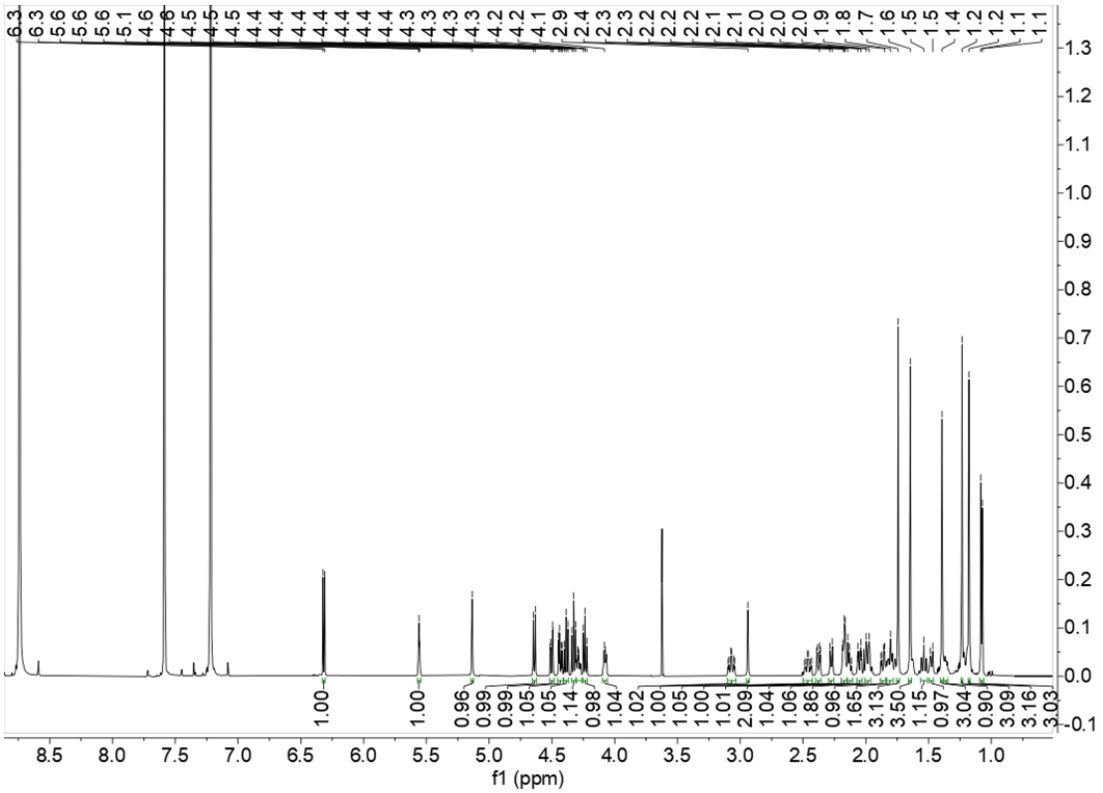

Figure S12. ^{13}C NMR spectrum (pyridine-d_5, 150 MHz) of compound **2**

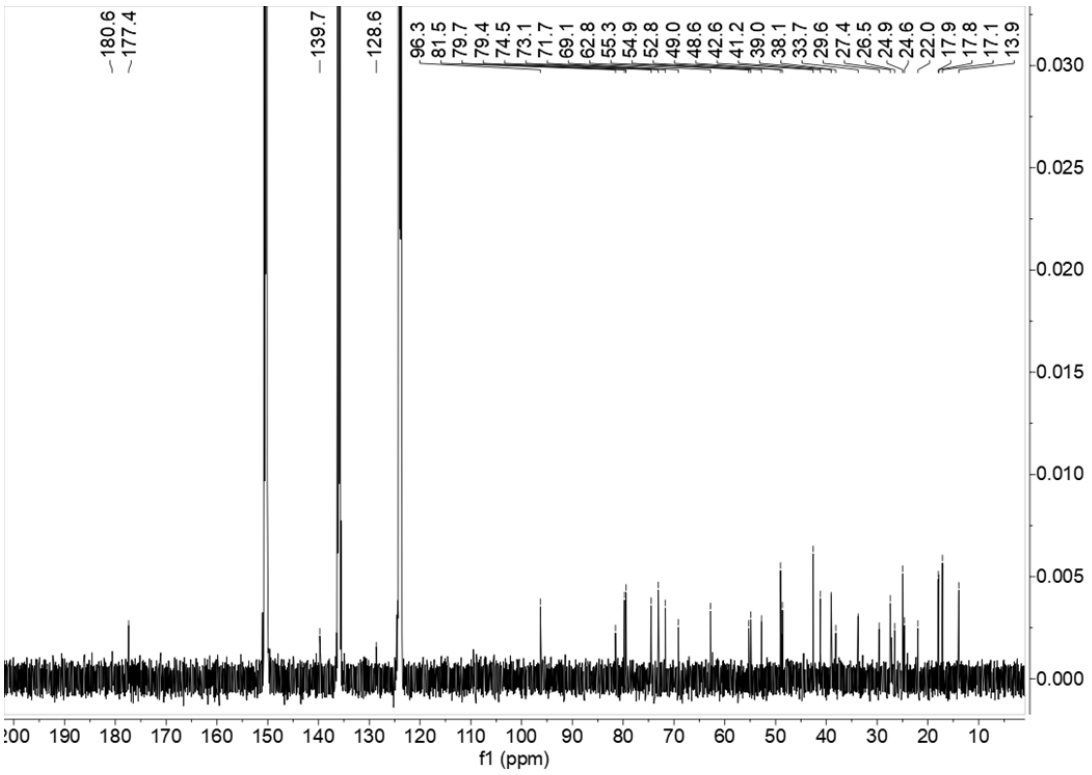

Figure S13. ^{1}H NMR spectrum (pyridine-d_5, 400 MHz) of compound **3**

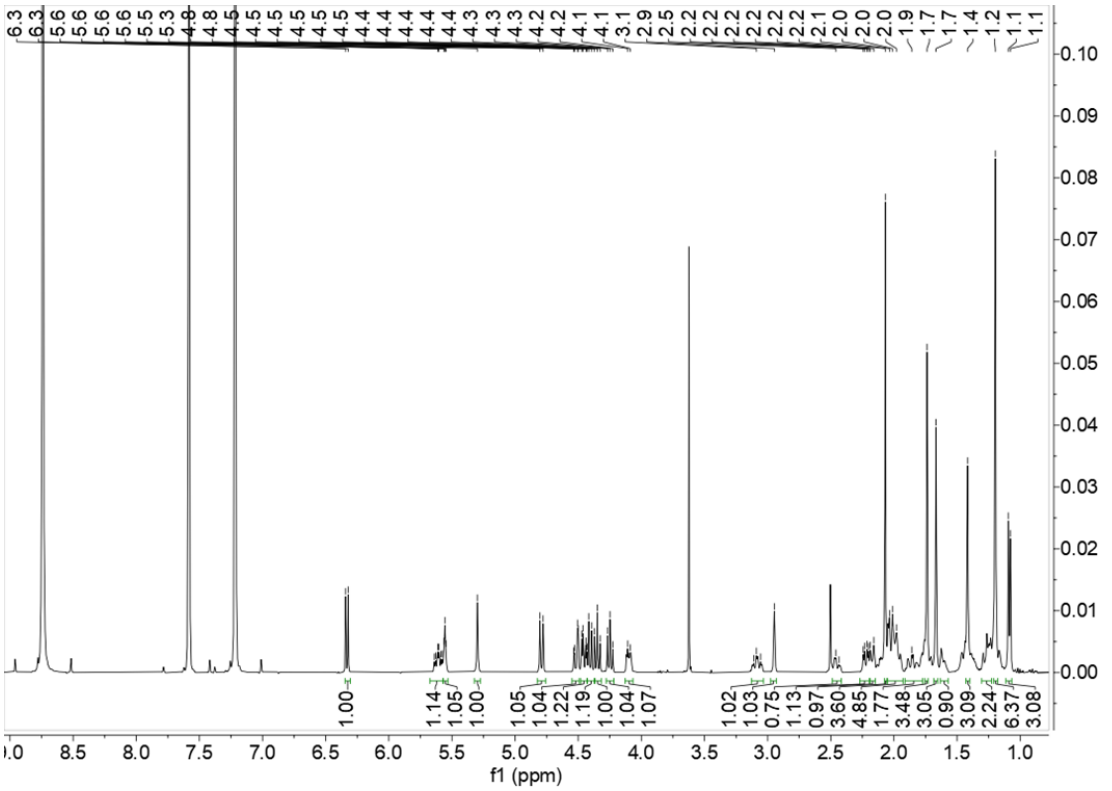

Figure S14. ^{13}C NMR spectrum (pyridine-d_5, 100 MHz) of compound **3**

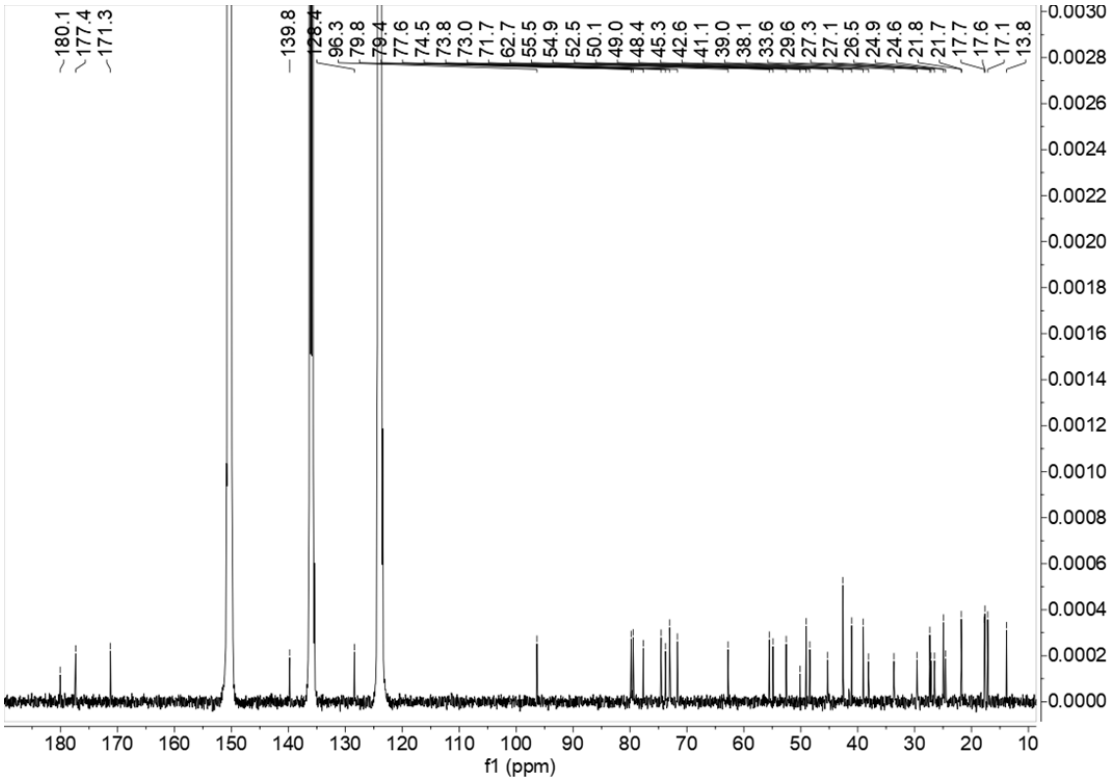

Figure S15. ^{1}H NMR spectrum (pyridine-d_5, 600 MHz) of compound **4**

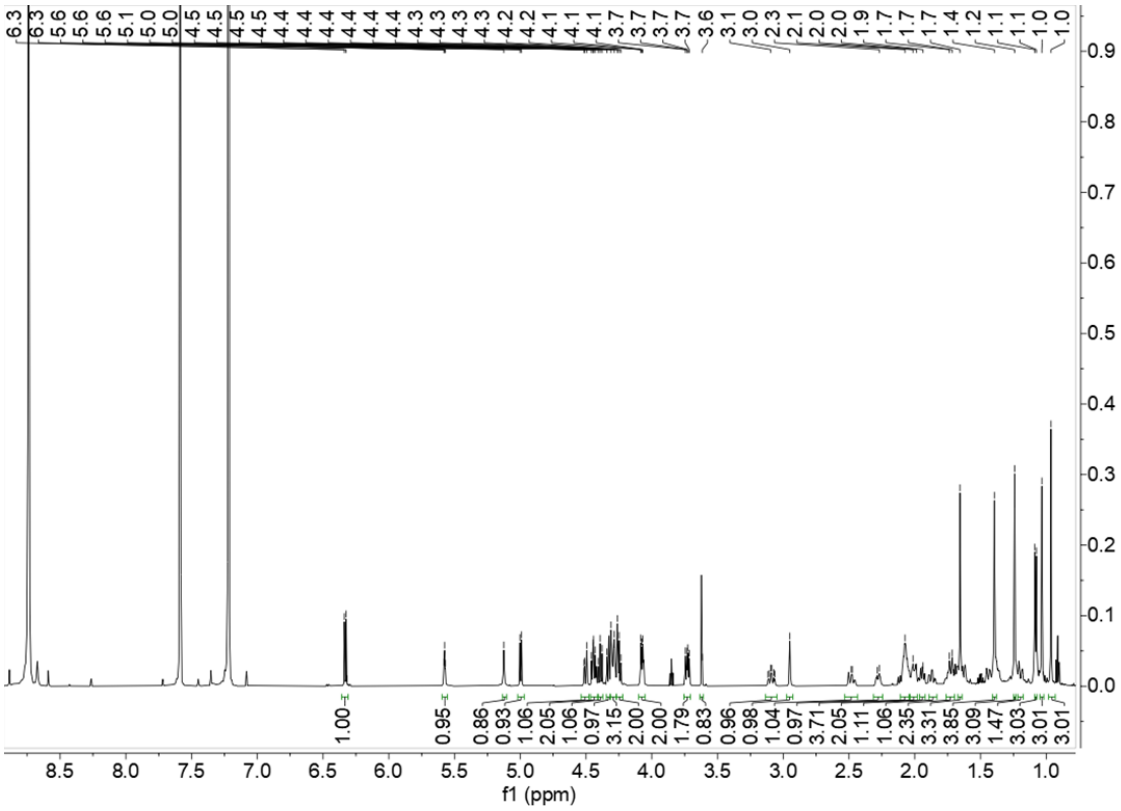

Figure S16. ^{13}C NMR spectrum (pyridine-d_5, 150 MHz) of compound **4**

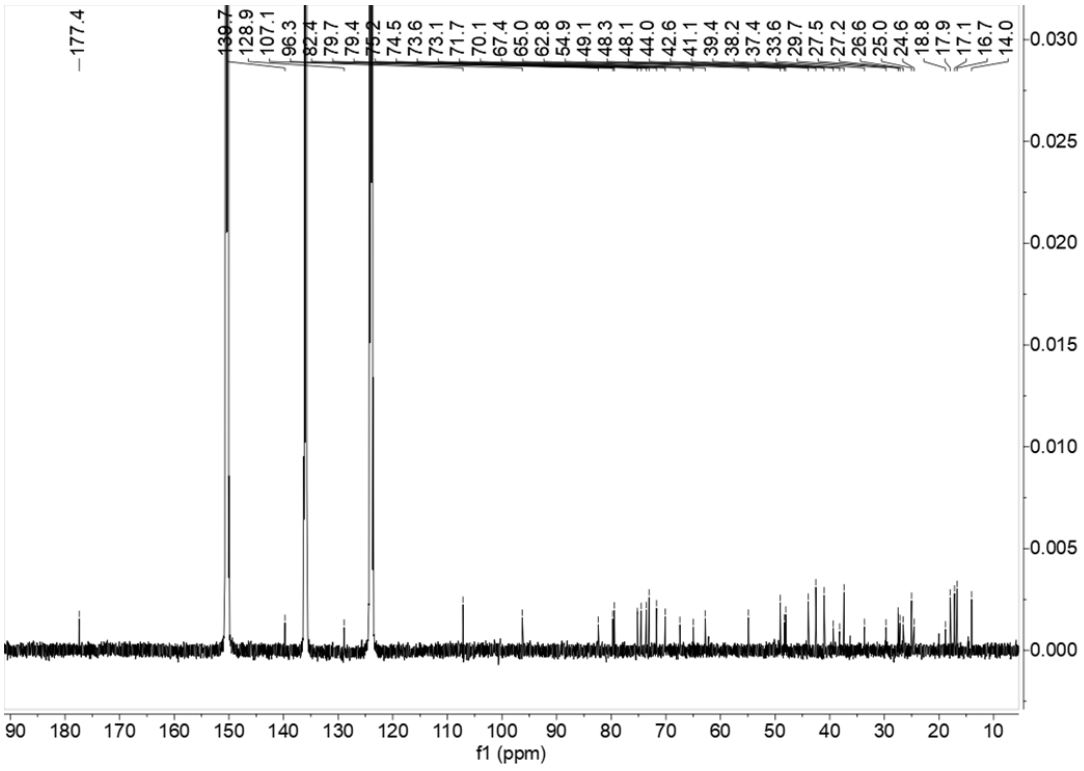

Figure S17. ^{1}H NMR spectrum (pyridine-d_5, 400 MHz) of compound **5**

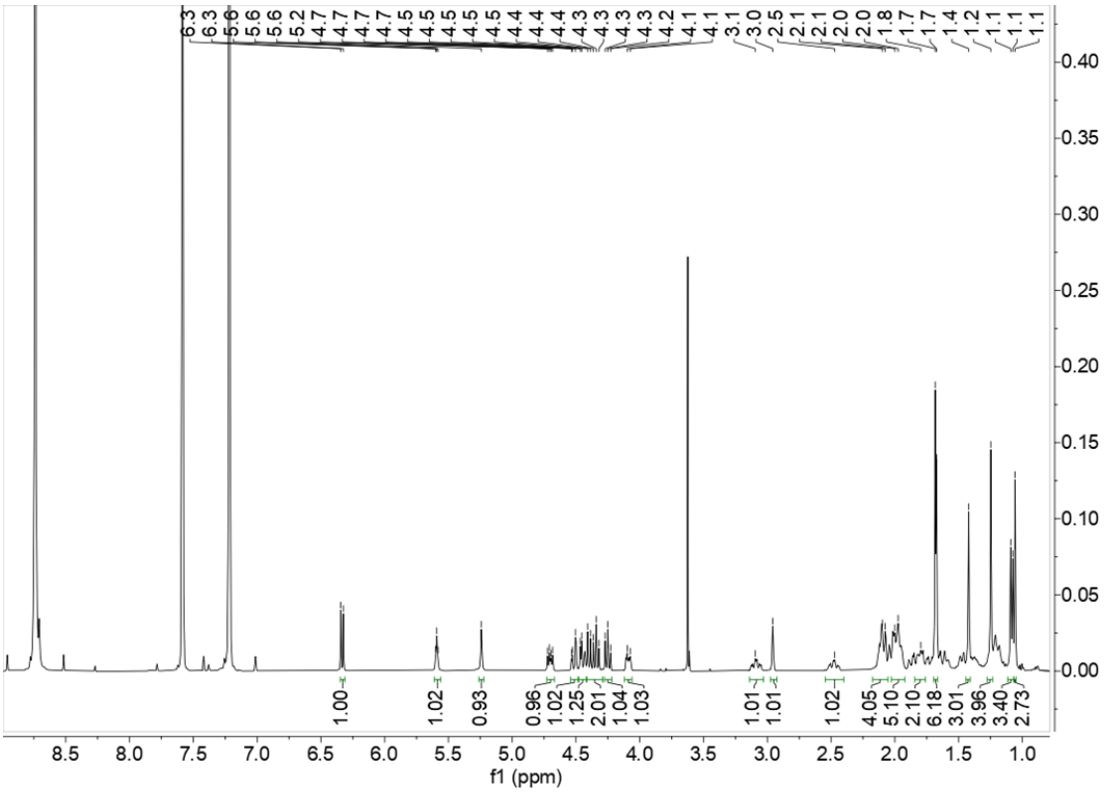

Figure S18. ^{13}C NMR spectrum (pyridine-d_5, 100 MHz) of compound **5**